

NANO AND MICROSTRUCTURE EFFECTS ON THE BIOACTIVITY OF FORSTERITE POWDERS

M. GOREA*, #M-A. NAGHIU*, M. TOMOAI-A-COTISEL*, G. BORODI**

*Department of Chemical Engineering, "Babeş-Bolyai" University,
Arany Janos Str. no. 11, RO-400028, Cluj Napoca, Romania

**National Institute for R&D of Isotopic and Molecular Technologies,
65-103 Donath Str., RO- 400293, Cluj-Napoca, Romania

#E-mail: adriana_naghiu@yahoo.com

Submitted January 15, 2013; June 16, 2013

Keywords: Forsterite, Nano and micro powders, Bioactivity

Forsterite (Mg_2SiO_4) powder has been synthesized from talc ($Mg_3Si_4O_{10}(OH)_2$) and magnesium carbonate ($MgCO_3$) by applying solid state reactions method. The raw materials mixture has been milled for 10 hours until nano powders have been obtained. This mixture was then thermally treated at various temperatures. The synthesized material was structurally characterized by X-ray diffraction. Forsterite represented the main crystalline phase in the samples fired to 1100 and 1200°C, while at 1000°C small amounts of enstatite and periclase were still identified. The particles size and morphology were investigated by TEM, SEM and AFM, and the grain size distribution with a Counter Coulter-type laser granulometer. A ratio of 75 % of the particles in the samples fired to 1000, and respectively 1100°C were less than 25 nm, while the maximum size was 42 nm. For the samples fired at 1200°C, most of the particles (74 %) were larger, about 6.8 µm, with a maximum of 70 µm. In order to evaluate its bioactivity, we have immersed the forsterite powder into simulating body fluids (SBF). Following 28 days of experiment, the FTIR spectra collected on the forsterite nanopowder contained the specific hydroxylapatite bands, while in the case of the micro powder these bands are hardly visible.

INTRODUCTION

Modern technology requires new biomaterials with mechanical features similar to human bone [1-3]. Among these, ceramic materials have proved to be suitable for medical applications [4, 5].

Magnesium and silicium play an important role in human body processes. Recent research has shown that the compounds in the MgO–SiO₂ system are biocompatible, thus they are suitable to be used for dental and orthopaedic prosthetic materials [6-8].

The mechanical activation of the reaction mixtures has been, and still is often used for obtaining crystalline [9, 10] and composite [11, 12] materials in the nanometre range given the relatively low processing costs. Chemical reactions in mechanically-activated mixtures can be accelerated in the view of obtaining nanocrystalline powders with pre-established mineralogical composition [10, 13].

In comparison with micro particles, nanoparticles show increased diffusion rates, reduced heating time and temperature, with improved mechanical and biological properties [4, 14].

During forsterite synthesis, the formation of enstatite ($MgSiO_3$) and/or periclase (MgO) as secondary phases is almost impossible to constrain [10, 15]. It was ob-

served that thermal treatment at 1200°C or up to 1600°C is needed, in order to synthesize solely forsterite [16]. Because at 1557°C enstatite dissociates into forsterite and SiO₂-rich fluid, its presence may negatively influence the forsteritic ceramics' properties at high temperatures [17].

The aim of this research was the synthesis of forsterite *via* solid state reaction method and its physical and mineralogical characterization in the view of evaluating the potential of *in vitro* apatite formation on the particles composing the nano- and micropowders.

EXPERIMENTAL

Preparation of the forsterite nanopowder

The forsterite nanopowder was synthesized *via* solid phases reaction by using magnesium carbonate ($MgCO_3$) (98 % purity, Merck) and talc ($Mg_3Si_4O_{10}(OH)_2$) (98 % purity, Merck) as raw materials. In order to reach forsterite stoichiometry, Mg-carbonate and talc were mixed in an initial 5:1 molar ratio. The mixture was milled for 10 hours by using a Fritsch „pulverisette 6"-type planetary ball mill in order to provide an ideal mixing and mechanical activation. The mill body and the

12-mm balls are made of sintered alumina. It was used a 1.5:1 ball: material ratio, with 300 rpm rotation speed. Following milling, the mixture is thermally treated to 1000, 1100 and respectively 1200°C, with one hour constant heating regime at maximum temperature.

Characterisation of the forsterite powder

The diffraction data were collected in the $2\theta = 15-85^\circ$ angular domain with a Bruker D8 Advance diffractometer, using Cu $K\alpha_1$ radiation ($\lambda = 1.5406 \text{ \AA}$) (40 kV; 40 mA). In order to increase the resolution, a Ge 111 monochromator was used to eliminate the $K\alpha_2$ radiation.

The crystallite size was estimated from the X-ray diffractograms using the Scherrer formula [18], see equation 1:

$$D = \frac{k \lambda}{\beta_{1/2} \cos(\theta)} \quad (1)$$

where D is the crystallite size (\AA); k is a shape factor equal to 0.9; λ is the X-ray wavelength (1.5405 \AA); θ is the diffraction angle expressed in radians, and $\beta_{1/2}$ was calculated using equation 2:

$$\beta_{1/2} = \sqrt{B^2 - b^2} \quad (2)$$

where B being the diffraction peak width at half height and $b = 0.065$ the natural width of the instrument.

For this purpose, we have selected three individual, very well-differentiated peaks of highest intensity.

The size and shape of forsterite crystallites synthesized at 1100°C were investigated by transmission electron microscopy (TEM) on a JEOL-type JEM 1010 equipment. JEOL- customized software was used for analysing the TEM images. The crystallites morphology and grain size were also studied by scanning electron microscopy (SEM) on a JEOL 5600 LV unit and by atomic force microscopy (AFM) on a JEOL 4210 unit. A Shimadzu Sald-7101 Counter Coulter laser granulometer was used for investigating the grain size distribution.

The process of formation of hydroxylapatite on the surface of the forsterite powder was monitored by infrared (IR) spectroscopy on a FT-IR JASCO 6100 unit in the $4000-400 \text{ cm}^{-1}$ interval with 4 cm^{-1} resolution by using the KBr-pellets method.

In vitro evaluation of the powders bioactivity

The *in vitro* bioactivity of the forsterite powder has been investigated by placing it into simulating body fluids (SBF) for an interval ranging from 7 to 28 days. The solid: fluid ratio was 1.5 mg/ml, the fluid being not replaced meanwhile. The SBF fluid has been prepared according to the procedure in Kokubo and Takadama

[19]. The experimental setting was immersed into a water bath kept heated at 37°C. After well established reaction times, the powder was filtered and slightly washed with distilled water in order to remove the extra SBF solution, then the powder was dried at 100°C and analysed.

RESULTS AND DISCUSSIONS

Characterisation of the forsterite powder (phase composition)

Figure 1 illustrates the X-ray powder diffraction on forsterite powders synthesized at various temperatures: 1000, 1100 and respectively 1200°C.

The X-ray spectra document the formation of forsterite at 1000°C; nevertheless, even under advanced mechanical mixing the reaction is not complete. The spectrum also contains low-intensity peaks of enstatite and periclase. Also, a low crystallinity degree of forsterite is noticeable. One would assume that after 10 hours of milling the crystalline structure of the raw minerals has partly or totally collapsed, thus imprinting a faster reaction rate. The defects resulted *via* mechanical activation is expected to facilitate the MgO diffusion on the silica surface (10).

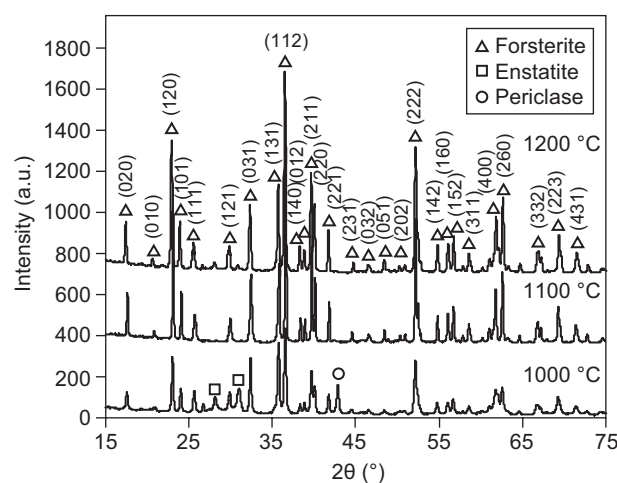


Figure 1. X-ray diffraction patterns on the experimental samples.

In the diffraction patterns of the samples heated at 1100 and respectively 1200°C the single crystalline phase is represented by forsterite. The absence of the characteristic peaks for the intermediary phases enstatite and periclase proves that, by advanced milling of the raw materials and increase firing temperature, the synthesized crystalline material contains solely forsterite. It can be summarized that the formation of forsterite under the given conditions is finalized at 1100°C.

The size of the crystallites in the powders obtained by firing at 1000°C, 1100°C and 1200°C was determined by applying the Scherrer equation. When the mixture was fired at 1000°C and 1100°C, the forsterite crystallites

were between 25 and 35 nm in size. Larger grains, *i.e.*, between 70 and 78 nm were measured for the sample synthesized at 1200°C.

Particle size distribution

The measured particle size distribution in the studied samples is illustrated in Figure 2. A single size interval, at almost identical absolute values, was noticed in the case of the samples fired at 1000°C and respectively 1100°C. In both samples, about 75 % particles are smaller than 25 nm, the maximum size being 42 nm. These values are close to the crystallite size calculated by using the Scherrer equation. An increase in grain size was noticed in the sample fired at 1200°C, 75 % of the grains being smaller than 6.8 µm. In this case, the maximum sizes are 70 µm. This effect is clearly a result of the presence of grain aggregates in this last sample.

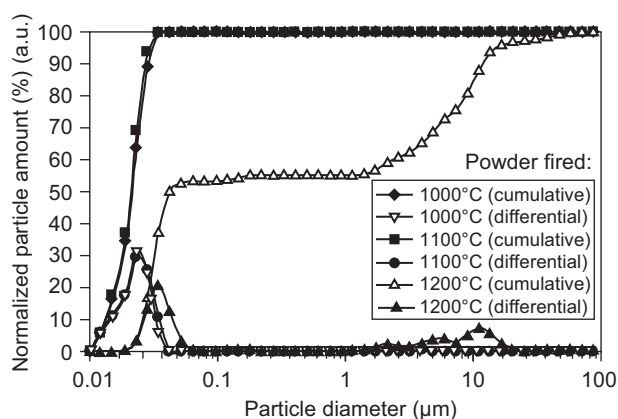


Figure 2. Grain size distribution in the forsterite powders synthesized at various temperatures.

Evaluation of the AFM results

The AFM study concerned the morphology of the forsterite powder obtained at three distinctive synthesizing regimes. We have measured the sample roughness on an area of $2.5 \times 2.5 \mu\text{m}$.

Besides the obvious surface roughness noticed in all the samples, the AFM images (Figure 3) confirm that the samples fired at 1000°C and 1100°C consist of nanometre grains, below 40 nm. In the sample fired at 1200°C, the grains are in the micrometers range, while the grain aggregates are clearly illustrated.

TEM microscopy results

Transmission electron microscopy was used for investigating the morphology and sizes of the crystallites in the powder synthesized at 1100°C (Figure 4). The graphs illustrate forsterite aggregates of grains with irregular shapes but sizes ranging in a narrow interval. The average size of the crystallites is 20 nm.

SEM microscopy

The SEM images on the forsterite powder obtained after 10 hours of mechanical activation and firing at 1000°C, 1100°C and 1200°C are presented in Figure 5.

The sample fired at 1000°C (Figure 5a) consists of small grains with low crystallinity. When the synthesis temperature increased at 1100°C, the crystallites developed better-evidenced morphologies, with no significant increase in grain size (Figure 5b). Figure 5c illustrates larger crystallites forming aggregates, in the sample fired at the highest experimental temperature (1200°C).

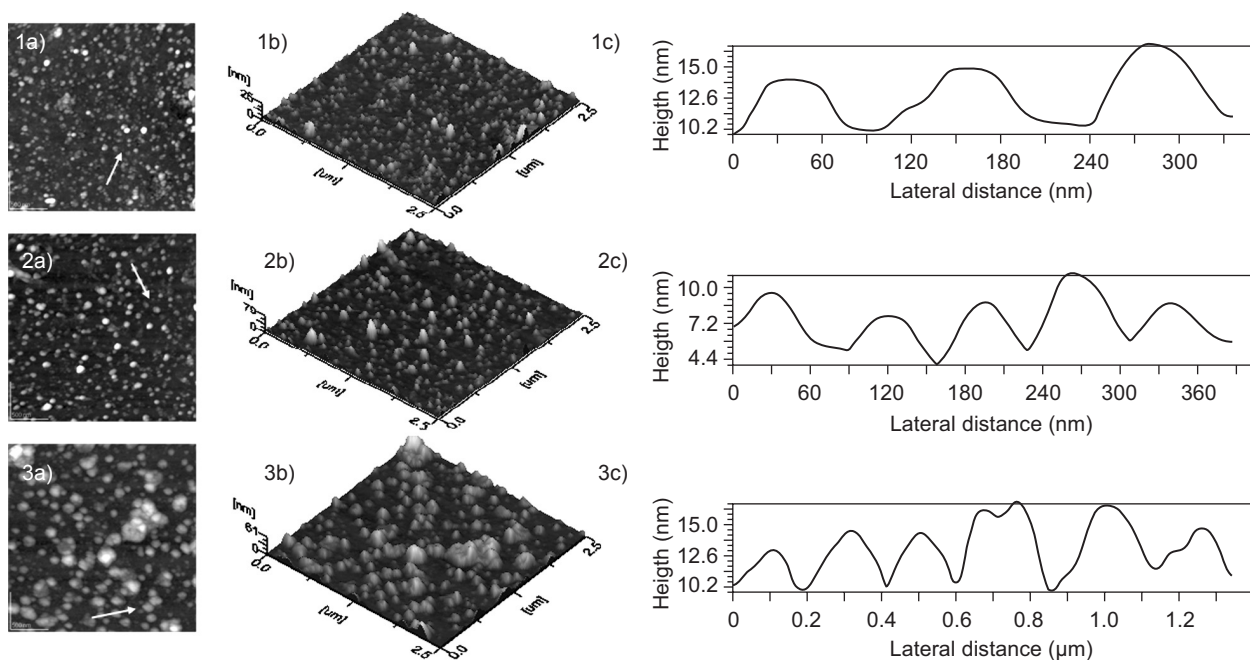


Figure 3. AFM images of the forsterite powder fired at 1) 1000°C; 2) 1100°C; and 3) 1200°C. Measured panel: $2.5 \mu\text{m} \times 2.5 \mu\text{m}$. a) 2D-topography; b) 3D-images of the panels c) cross section along the arrow in panels a)

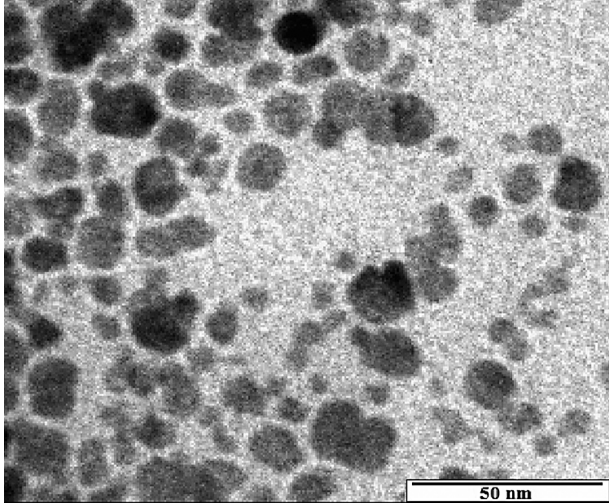
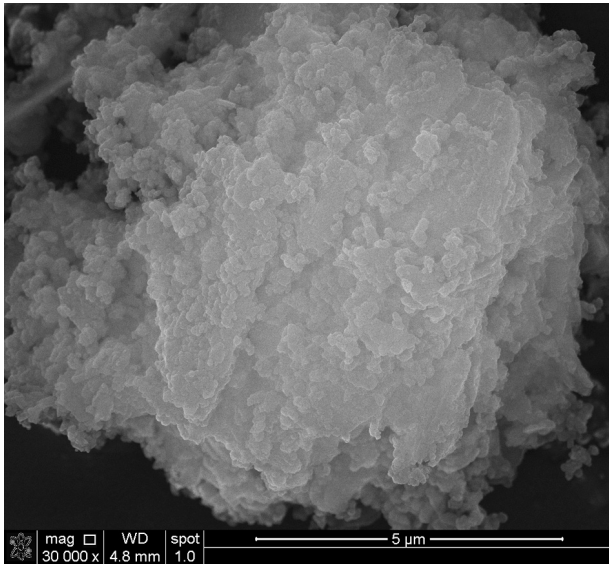
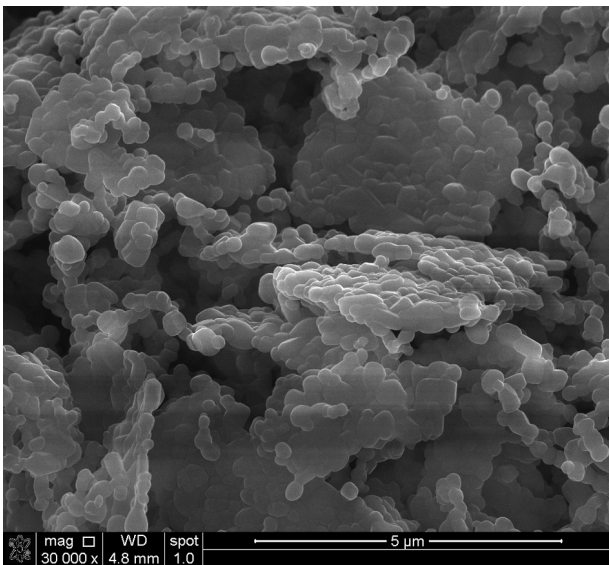


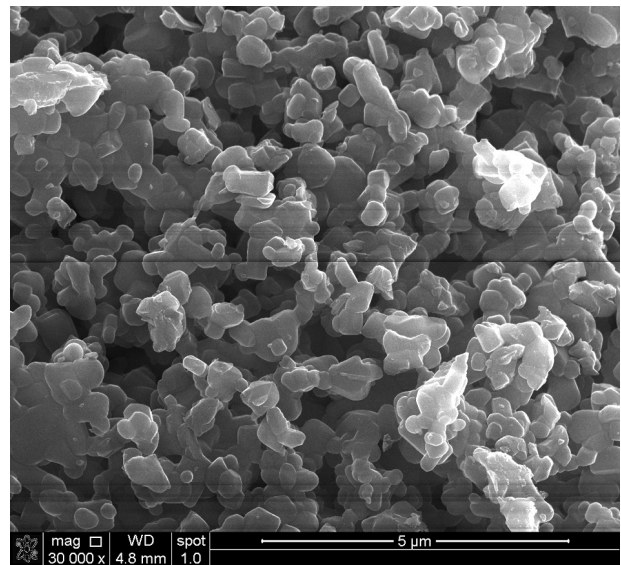
Figure 4. TEM image of the powder synthesized at 1100°C.



a) 1000°C



b) 1100°C



c) 1200°C

Figure 5. SEM images on the forsterite powders fired at 1000, 1100 and respectively 1200°C.

Evaluation of the in vitro bioactivity

In Figure 6 we plotted the FTIR spectra of the studied forsterite powders, before and after their immersion in the SBF fluid.

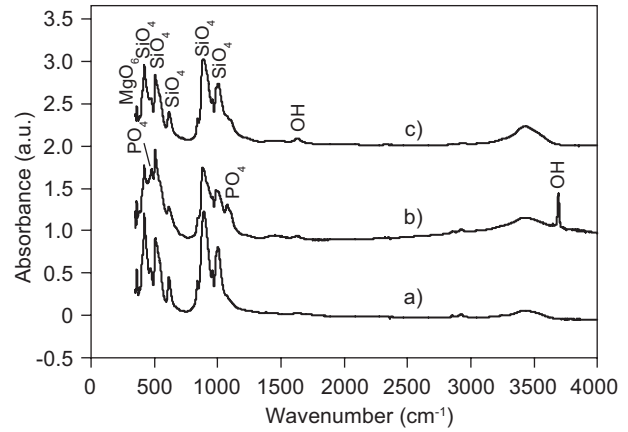


Figure 6. FTIR spectra of the forsterite powders: a) sample fired at 1100°C, before immersion in SBF; b) and c) sample fired at 1100°C and 1200°C respectively and immersed in the SBF fluid for 28 days.

The typical forsterite bands, located at 420 cm^{-1} - representing the MgO_6 group, at 513 and 620 cm^{-1} - representing the SiO_4 bending, and at 890 and 1010 cm^{-1} - representing the SiO_4 stretching are present in the spectrum collected before the immersion into SBF.

After 28 days of immersion of the nanopowder sample fired at 1100°C into the SBF solution, new bands assigned to O-H, C-O and P-O are noticeable in the FTIR spectra. Very distinctive are the OH-bond absorption bands at 1660 cm^{-1} , 3450 cm^{-1} and 3690 cm^{-1}

related to the newly-formed hydroxylapatite. At the same time, new absorption bands occur at 496 cm^{-1} and at 1074 cm^{-1} , corresponding to the PO_4 group. Thus, one can conclude that after 28 days of immersion in SBF hydroxylapatite forms on the forsterite nanograins [2].

In the case of the sample synthesized at 1200°C showing micrometer-size grains, only the typical forsterite bands and the one of OH-group at 1660 cm^{-1} are visible; the PO_4 bands are hardly evidenced in the spectra. As a summary, it can be stated that micrometer-range grains of forsterite show less ability to support hydroxylapatite formation, as compared to the nanopowder.

CONCLUSION

The forsterite powder was prepared by using the solid state reaction method starting from magnesium carbonate and talc, followed by thermal treatment at 1000, 1100 and 1200°C . As proven by the X-ray diffraction patterns, the reaction of formation of the forsterite nanopowder is completed after mechanical activation for 10 hours and firing at 1100°C . TEM and SEM microscopy evidence the formation of nanocrystallites of irregular shapes that sometimes form aggregates. The AFM analysis confirms the nanometre-size range of the crystallites for the powders fired at 1000°C and respectively 1100°C , and illustrates the formation of thin films with the rough surfaces. The investigation of the grain size distribution (by Counter Coulter method) indicated nanometre-sized forsterite grains in the sample fired at 1000 and 1100°C , with most of the grains below 40 nm in size. Grain sizes are larger, micrometer in size, in the case of the sample synthesized at 1200°C mainly as a result of grain aggregation processes.

The FTIR results clearly demonstrate the formation of hydroxylapatite on the nanometre-sized forsterite grains after 28 days of immersion in the SBF fluid. At the same time, this process is less evident in the case of the larger, micrometre-sized powders. The *in vitro* bioactivity tests show a good bioactivity reaction for the synthesized forsterite nanopowders. Thus, they can be successfully used as biomaterials in the remediation of bone tissue.

Acknowledgment

This work was financially supported by research project 171/2012. One of the authors (M. A. Naghiu) thanks the financial support of the Sectoral Operational Programme for Human Resources Development 2007-2013, co-financed by the European Social Fund, under the project number POSDRU/107/1.5/S/76841, with the title „Modern Doctoral Studies: Internationalization and Interdisciplinarity”.

References

1. Tavangarian F., Emadi R.: *Ceramics International* 37, 2275 (2011).
2. Tavangarian F., Emadi R.: *Materials Letters* 65, 740 (2011).
3. Regi M. V., Calbet J.M.G.: *Prog. Solid State Chem.* 32, 31 (2004).
4. Ghomi H., Jaberzadeh M., Fathi M.H.: *J. Alloys Compd.* 509, L63 (2011).
5. Oh S., Oh N., Appleford M., Ong J.L.: *Am. J. Biochem. Biotechnol.* 2, 49 (2006).
6. Kharaziha M., Fathi M. H.: *Ceramics International* 35, 2449 (2009).
7. Kharaziha M., Fathi M.H., *Journal of mechanical behaviour of biomedical materials* 3, 530 (2010).
8. Siyu N., Lee C., Jiang C., *Ceramics International* 33, 83 (2007).
9. Suryanarayana C.: *Progress in Materials Science* 46, 1 (2001).
10. Tavangarian F., Emadi R., *Ceramics - Silikaty* 54, 122 (2010).
11. Fabing Li, Lijun Jiang, Jun Du, Shumao Wang, Xaiopeng Liu, Feng Zhan: *J. Alloys Compd.* 452, 421 (2008).
12. Maiti R., Chakraborty M.: *J. Alloys Compd.* 458, 450 (2008).
13. Takacs L.: *Prog. Mater. Sci.* 47, 355 (2002).
14. Fathi M.H., Kharaziha M.: *Materials Letters* 63, 1455 (2009).
15. Tavangarian F., Emadi R., Shafyei A.: *Powder Technology* 198, 412 (2010).
16. Tavangarian F., Emadi R.: *Journal of Alloys and Compounds* 485, 648 (2009).
17. Douy A.: *J. Sol-Gel Sci. Technol.* 24, 221 (2002).
18. H. P. Klug, L. E. Alexander: *X-Ray Diffraction Procedures*, p. 655, John Wiley & Sons, New York, 1974.
19. Kokubo T., Takadama H.: *Biomaterials* 27, 2907 (2006).